On Effective Virtual Inertia of Storage-Based Distributed Control for Transient Stability

Eman Hammad, *Student Member, IEEE*, Abdallah Farraj, *Member, IEEE*, and Deepa Kundur, *Fellow, IEEE*

***Abstract*—In this paper, we consider a distributed energy storage system (ESS)-based control paradigm for transient stability of power systems. Utilizing a multi-agent control framework, we propose an effective virtual inertia measure for cyber-physical agents that includes both traditional synchronous generators and actuated ESSs. We derive the effective virtual inertia analytically for the case of general ESS-based control. We further consider the case of parametric feedback linearization control (PFL) as an application and investigate the proposed inertia measures after applying the PFL control. The utility of the proposed inertia measures is studied using the IEEE 68-bus test power system. Numerical results demonstrate the impact of storage limits, control scheme aggressiveness, and delay on the proposed inertia measures during a disturbance in the power system.**

***Index Terms*—Cyber-physical agent, smart grid, feedback linearization control, transient stability, multi-agent framework, inertia, energy storage, distributed control.**

I. Introduction

ADVANCEMENTS in power systems are unfolding as it continues to incorporate more renewable energy resources, energy storage systems as well as cyber-enabled and connected components. Energy storage systems (ESSs) are becoming popular in power systems with various applications ranging from stability and frequency regulation to energy economics. An ESS is a device that can be used to store energy which can be injected into the system for a variety of reasons. Power systems are also becoming more cyber-connected as a greater number of sensors is deployed and connected to control centers through communication networks. These advancements motivate designing new distributed ESS-based control paradigms to change power system dynamics.

Power system stability is the ability of the system to regain a state of operating equilibrium after being subjected to a physical disturbance [1]. A power transmission system is considered stable if, for example, the synchronous machines of the system return to a stable steady state operating point after the occurrence of a disruptive event. Transient stability refers to the ability of a power system to maintain its synchronism when subjected to a severe disturbance, such as the loss of a generation unit. Faults, and switching attacks can trigger transient instability in power systems.

Classical approaches for transient stability control relied on fast clearance of the fault using fast-acting circuit breakers to trip the faulted transmission lines. Further, automatic power control regulators are typically used to affect the excitation and governor systems of a synchronous generator to help restore synchronism. Finally, if a generator is not in synchronism, out-of-step protection systems are triggered to trip the affected generator [2]. To help enhance transient stabilty control and to avoid tripping of generators, recent studies have capitalized on the smart grid paradigm by proposing novel distributed control approaches. For example, a popular body of research is emerging that focuses on ESS-based distributed control that aims to enhance stability in power systems [3]–[7]. The resulting controllers actuate distributed ESSs to inject and/or absorb power from the system during and after disturbances in order to shape the dynamics of the power system to maintain or regain stability. A distributed transient stability control technique is often activated to address both accidental faults or targeted attacks on the grid. The response time of prime movers power control for a large hydro plant can range from few seconds to minutes, whereas the response time for actuated (fast-reacting) ESS is few cycles. Thus, the fast response of controlled ESS such as flywheels makes them adequate to address transient stability problems.

Power grid inertial response, resulting from the rotating masses of traditional generation machines, have been essential in characterizing the dynamical behavior of the grid and its stability [8]. Nevertheless, the increased penetration of low/zero inertia renewable generation into the grid is affecting the grid inertia and its stability characteristics. This has motivated the development of *virtual synchronous generators* (VSGs) that provide *virtual inertia* to the power grid and hence improve its stability properties. VSGs represent a power-electronics/converter control approach to emulate the behavior of synchronous machines over short periods of time [9]–[11]. Here, a VSG is comprised of a (typically low/zero inertia) distributed generator and a short-term energy storage device with a power inverter that is appropriately controlled to improve the dynamic response of the power system. Several works have recently proposed a variety of virtual-inertia control approaches for frequency regulation specially

Manuscript received January 10, 2017; revised April 10, 2017 and July 5, 2017; accepted July 31, 2017. Date of publication August 11, 2017; date of current version December 19, 2018. This work was supported by the Natural Sciences and Engineering Research Council of Canada under Grant RGPIN 227722. Paper no. TSG-00045-2017. *(Corresponding author: Eman Hammad.)*

The authors are with the Department of Electrical and Computer Engineering, University of Toronto, Toronto, ON M5S 3G4, Canada (e-mail: ehammad@ece.utoronto.ca; abdallah@ece.utoronto.ca; dkundur@ece.utoronto.ca).

Color versions of one or more of the figures in this paper are available online at http://ieeexplore.ieee.org.

Digital Object Identifier 10.1109/TSG.2017.2738633

for microgrids or power systems with high penetration of renewables [12]–[17].

Previous analysis of ESS-based control paradigms focused on the control design through optimizing control objectives and ESS resources for desired system dynamics. While this approach provided a working framework that considered in some cases optimal virtual inertia introduced by the storage, it did not provide tools or measures to capture the aggregate effect of the storage and its associated distributed control. Moreover, traditional measures of system performance such as angular frequency reflect the system dynamics but not the effective performance of the ESS-based control. Hence, this motivates the need to define new measures to describe the inertial response of the ESS and its associated control and provide direct design insights.

In this article we draw an analogy between the role of distributed control for transient stability and physical inertia in synchronous generators, both, aimed at improving transient stability. Therefore, we reintroduce the notion of *virtual inertia* as a result of ESS-based distributed control. Then we consider a collective cyber-physical *effective* virtual inertia paradigm that quantifies the combined effect of a distributed control agent actuating an ESS for the purpose of transient stability of an associated synchronous generator. The proposed measures appear as time varying quantities that reflect the agent operation, control, ESS characteristics and dynamics. We apply the proposed measures on a state-of-art ESS-based distributed control as an application. We consider parametric feedback linearization (PFL) control [3], [7] for its simple tunable design that allows for tractable advanced analysis.

While previous research has developed inverter-based ESS-actuating controls to emulate a VSG, in this work we consider a different perspective. A general distributed control for transient stability with a general control objective that actuates an ESS is considered. For this general ESS-based control we analytically describe the effective inertia as a function of the parameters and characteristics of the control and the associated ESS. We assert that the framework and associated metrics facilitate the study of ESS-based distributed control and its impact on system dynamics. Further, within this framework the proposed effective virtual inertia measure relies on the cyber-physical operation of the distributed control agent, and thus we are able to study the metric in relation to smart grid communication latency, ESS capacity and control structure and parameters. We provide analytical and numerical insights.

A. Problem Statement

We model the power system as a multi-agent cyber-physical system comprised of N agents [5], [7]. In this representation, each cyber-physical agent is composed of: 1) a synchronous generator, 2) a sensor that provides local measurements of the generator rotor angle and speed, 3) a distributed controller that processes sensor data from system agents, and 4) a fast-acting ESS (such as a flywheel) that can inject or absorb real power in the system depending on the value of the control signal. In this model, a communication network connects the different cyber-physical agents. The controller (also referred to as control agent) affects the dynamics of the power system by actuating the local fast-acting ESS entity.

In this model, the physical dynamics of each cyber-physical agent depend on its own state as well as the states of other agents in the system. The sensors, distributed controllers, and associated communication infrastructure form the *cyber* components of the multi-agent system; whereas, the synchronous generators and associated power system devices including the ESSs represent the *physical* elements of this system. The system agents are connected physically through transmission lines and buses and in cyber form through the communication network.

The distributed controller employed at each Agent i, where $i \in \{1, \ldots, N\}$, actuates the ESS using a computed control signal u_i to improve system stability. We assert that this ESS-based control acts as an effective *virtual inertia* on the closed-loop dynamics akin to the physical inertia of synchronous generators. We aim to describe the inertial response of the cyber-physical agent i as a function of the control signal u_i, where u_i captures the ESS related characteristics. We introduce the notion of effective virtual inertia to describe the inertial response of the agent and investigate its significance in evaluating the collective effect of both physical and cyber mechanisms for enhancing transient stability.

B. Contributions

The main contributions of this work include:

1) proposing the concept of "effective virtual inertia" in the context of ESS-based distributed control for transient stability;
2) deriving a general analytical expression for the effective virtual inertia measure for two system-level components: a) the cyber-physical agent consisting of the synchronous machine, an ESS and its control operation, and b) the actuated ESS alone; and
3) studying the potential of PFL control within the proposed inertia-based paradigm.

The remainder of this manuscript is organized as follows. Relevant background on stability and dynamics and the problem setting are presented in Section II. The developed inertia measures are presented in Section III and are detailed in Section IV for the case of PFL control. Section V numerically investigates the proposed measures and considers non-ideal cyber-physical conditions. Finally, conclusions are presented in Section VI.

II. Control for Transient Stability

A. Power System Stability

Physical disturbances on power system operation are often classified as either small or large [1]. Small disturbances include incremental load changes, while large disturbances are of a necessarily severe nature and include transmission line faults and loss of generation units. Power system stability is traditionally defined as the ability of the system to regain a state of operation equilibrium after being subjected to a physical disturbance [1]. Following the disturbance, if the power system is stable, it will either reach a new equilibrium state or

return to the original operating condition. Stability of power systems is of a great concern to system operators.

Rotor angle stability refers to the ability of the synchronous machines in a power system to remain in *synchronism* after being subjected to a disturbance [18]. This type of stability depends on the ability of a synchronous generator to maintain or restore balance between its electromagnetic and mechanical torques. If the power system has a rotor angle instability issues, then some synchronous generators may experience increasing angular swings which may lead to loss of synchronization amongst the different generators in the system.

When the power system is in a steady and secure state, there is a balance between the mechanical and electromagnetic torques of synchronous generators which leads to the rotor speed of each generator being constant. However, when there is an imbalance between the mechanical and electromagnetic torques, the rotor experiences an acceleration or deceleration depending on the sign and degree of torque difference. Transient stability describes the ability of the power system to remain in synchronism when subjected to large disturbances [18]. The time frame of related studies is typically on the order of 3 to 5 seconds following a disturbance, and may extend to 10 or 20 seconds for large power systems [1]. Through application of control techniques, transient stability can be achieved after the occurrence of a physical disturbance by maintaining both speed synchronization and phase angle cohesiveness. Speed synchronization requires the rotor speed of generators to converge asymptotically to a common value. Phase angle cohesiveness refers to the property whereby the differences between the rotor phase angle of the different synchronous generators of the power system are below a predefined threshold.[1]

Given our focus, in this work, on addressing issues of transient instability, we employ the well-known swing equation model of synchronous generators to describe power system dynamics. The swing equation links the rotor angle and speed of a synchronous generator to enable the study of transient stability. In addition, a Kron-reduction technique [20] is employed to efficiently model the physical power grid interconnections to determine effective admittance-based mutual couplings. In conjunction with the swing equation model of each generator, an additional set of coupled differential equations can be used to represent the overall transient stability dynamic behavior of the power system.

B. Power System Dynamics

Consider a power system consisting of N synchronous generators. For the ith generator, where $i \in \{1, \ldots, N\}$, the generator parameters and states are listed in Table I. The two-axis sub-transient machine model is widely used to capture the dynamics of synchronous generators during transients. In this model, the electrical dynamics of Generator i's stator are

TABLE I
MACHINE PARAMETER DESCRIPTION

Parameter	Description
δ	rotor angle
ω	rotor angular speed
ω_s	synchronous speed
D	damping coefficient
E'_d	d-axis transient electromotive force (emf)
E'_q	q-axis transient emf
E_f	field voltage
H	machine inertia constant
I_d	d-axis component of stator current
I_q	q-axis component of stator current
R_a	armature resistance
X_d	d-axis synchronous reactance
X_q	q-axis synchronous reactance
X'_d	d-axis transient reactance
X'_q	q-axis transient reactance
T'_d	d-axis transient open loop time constant
T'_q	q-axis transient open loop time constant
T_E	electromechanical torque
T_M	mechanical torque
V_d	d-axis terminal voltage
V_q	q-axis terminal voltage

represented as [21], [22]:

$$\dot{E}'_{qi} = \frac{1}{T'_{di}}\Big(-E'_{qi} - \big(X_{di} - X'_{di}\big)I_{di} + E_{fi}\Big) \tag{1}$$

$$\dot{E}'_{di} = \frac{1}{T'_{qi}}\Big(-E'_{di} + \Big(X_{qi} - X'_{qi}\Big)I_{qi}\Big) \tag{2}$$

$$E'_{qi} = V_{qi} + R_{ai}I_{qi} + X'_{di}I_{di} \tag{3}$$

$$E'_{di} = V_{di} + R_{ai}I_{di} - X'_{qi}I_{qi} \tag{4}$$

where $\dot{E}'_{qi}$ and $\dot{E}'_{di}$ denote the time derivative of E'_{qi} and E'_{di}, respectively. Let Ω_s denote the system frequency (typically equal to $60 \cdot 2\pi$ or $50 \cdot 2\pi$ depending the geographical location). the rotor dynamics of the synchronous generator can be expressed by [21]:

$$\dot{\delta}_i = \Omega_s(\omega_i - \omega_s) \tag{5}$$

$$\dot{\omega}_i = \frac{\omega_s}{2H_i}(T_{Mi} - T_{Ei} - D_i(\omega_i - \omega_s)) \tag{6}$$

where $\dot{\delta}_i$ and $\dot{\omega}_i$ are the time derivatives of δ_i and ω_i, respectively.

Further, the field voltage of a generator is controlled by the excitation control system, while the mechanical torque is controlled by the governor. The electromechanical torque is calculated as [21]:

$$T_{Ei} = E'_{di}I_{di} + E'_{qi}I_{qi} + \Big(X'_{qi} - X'_{di}\Big)I_{di}I_{qi}. \tag{7}$$

Let P_{Mi} and P_{Ei} be the mechanical and electrical powers of Generator i, respectively, where $P_{Ei} = T_{Ei}$ and $P_{Mi} = T_{Mi}$ when using per units. Then, the dynamics of the rotor speed in relation to the mechanical and electrical powers (in per unit) is modeled as:

$$\dot{\omega}_i = \frac{\omega_s}{2H_i}(P_{Mi} - P_{Ei} - D_i(\omega_i - \omega_s)). \tag{8}$$

The *swing equation* model presented in (5) and (6) describes the electromechanical dynamics of the synchronous generator's rotor, which is useful for studying the behavior of

[1]For a two-machine power system this threshold is determined based on the equal-area criteria and is found to be 180°− (initial rotor angle difference between the two generators) [19].

synchronous generators when the power system is subjected to a large disturbance. Let $P_{Ai} = P_{Mi} - P_{Ei}$ refer to the accelerating power of Generator i, $\forall i \in \{1, \ldots, N\}$. Typically $P_{Ai} = 0$ during normal operations. However, when a major disturbance occurs in the power system, the accelerating power of some generators deviates from 0. If a generators accelerating power is positive (negative), the generator's rotor will increase (decrease) its speed. Different traditional control schemes (such as excitation and governor control systems) accompany synchronous generators in order to respond to various disturbances; however, such traditional control systems exhibit slow reaction to rapid changes in the system dynamics. Fast reacting ESS and the availability of communication provided a good environment to develop advanced control paradigms to help enhance transient stability.

A large deviation in rotor speed may damage the synchronous machine if not tripped by out-of-step protection [18].[2] Consequently a generator might be disconnected from the power grid. A generator is said to be stabilized if its rotor speed is driven back to an acceptable range and when the rotor phase angle differences of the different synchronous generators are below a predefined threshold. Hence, the primary goal of control addressing transient stability is to intervene quickly to prevent out-of-step tripping of generators until other control mechanisms such as governors are functioning and can drive the system to stability. Transient stability of a power system can be evaluated using metrics that are indicative of the impact of the contengencies on the system dynamics [25]. The power angle-based stability index η can be evaluated as

$$\eta = \frac{360 - \delta_{\max}}{360 + \delta_{\max}} \tag{9}$$

where $\delta_{\max}$ is the maximum angle separation between any two generators in the system [25]. A higher value of η corresponds to a more favorable stability condition.

C. Distributed Control for Transient Stability

The goal of a transient stability control is to regain a balance between the mechanical and electromagnetic torques of a synchronous generator leading to constant rotor speeds. Thus, through the actions of the controller, synchronism is restored between the different generators in the system and rotor speed of the generators is driven to within an acceptable range.

Advanced distributed control schemes require the presence of cyber infrastructure to communicate the system state information. Sensor readings are periodically communicated to distributed controllers that affect the power system dynamics through power injection and absorption via ESSs. An ESS is a device that can store energy, and is able to absorb and inject electric power into the power grid. Available ESS technologies include flywheels, thermal, pumped hydro, solid state, compressed air, and capacitor systems.

The distributed control scheme can affect the dynamics of the power system by absorbing or injecting a specified amount of real power through the application of a fast-acting ESS at a designated generator bus. Incorporating the ESS actuation, described via u_i, at the bus of Generator i modifies the swing equation at time t to:

$$\begin{aligned} \dot{\delta}_i(t) &= \Omega_s(\omega_i(t) - \omega_s) \\ \dot{\omega}_i(t) &= \frac{\omega_s}{2H_i}(P_{Ai}(t) - D_i(\omega_i(t) - \omega_s) + u_i(t)). \end{aligned} \tag{10}$$

The transient stability control first addresses rotor speed deviations. Once rotor speed is stabilized, then the rotor angle differences between system generators become constant.

The ESS output is controlled in [4] depending on the level of frequency deviation in the power system. Nonlinear flocking-based control scheme was proposed in [5] to resynchronize the generators after the occurrence of a severe disturbance. Further, mechanical power of the generators is modulated in [26] to regulate the rotor speed. In addition, a PFL control scheme is proposed in [3], [6], and [7] for transient stability.

III. Inertia of Agents and ESS

Stability time refers to the time it takes a distributed controller to stabilize the associated generator, and it is traditionally used as a measure to quantify the performance of control schemes for transient stability applications. However, in this section we propose a different measure that mimics the inertia constants of synchronous generators.

A. Background on Generator Inertia

The swing model of a synchronous machine, as shown in (10), captures the basic dynamics of the synchronous machine where the combined inertia of the generator and its prime mover is accelerated by the imbalance between mechanical and electrical torques [18]. In other words, the machine rotational inertia represents a measure of its resistance to changes in rotational speed [15]. The development of the swing model incorporates the equation of rotational motion as:

$$J\frac{\mathrm{d}\omega_m}{\mathrm{d}t} = T_a = T_M - T_E \tag{11}$$

where J denotes the combined moment of inertia of the generator and turbine. Eq. (11) is then normalized in terms of the per unit inertia constant H, with a rated angular speed ω_{0m} and system rated power of VA_{base}, as:

$$J = \frac{2H}{\omega_{0m}^2} VA_{\text{base}}. \tag{12}$$

Noting that the rated torque is calculated as $T_{\text{base}} = VA_{\text{base}}/\omega_{0m}$, the per unit equation of motion becomes in the form of (6) [18].

We note that a synchronous machine's rotational inertia constant is a positive quantity that is related to the time constant of the machine dynamics; here, a lower value of inertia implies that a stable (unstable) synchronous machine is *easier* to destabilize (stabilize). This motivates our proposed "effective" inertia analogy for an agent, whereby a smaller effective inertia measure indicates that during a disturbance, an agent stabilizes more easily (i.e., faster). Hence, a synchronous machine's moment of inertia models the mechanical

[2]Example settings for out-of-step tripping protection in a multi-machine system can be found in [23] and [24].

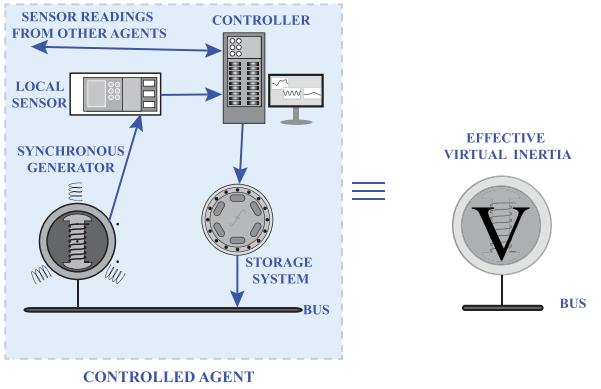

Fig. 1. Effective inertia of an agent.

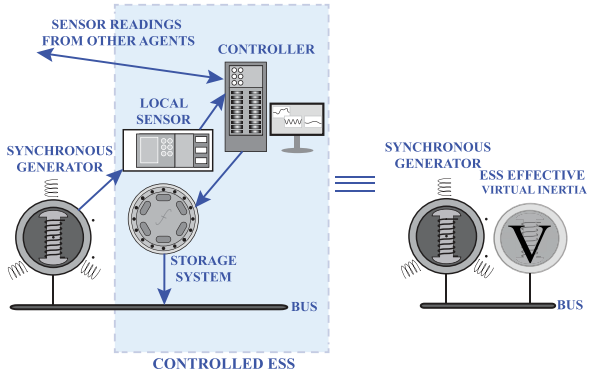

Fig. 2. Effective inertia of an actuated ESS.

inertia of the machine which relates to its rotational dynamics. Our source of proposed virtual inertia, on the other hand, *emulates* inertia by imposing defined control actions adhering to the swing model dynamics. Subsequently, we assert that the proposed effective inertia measure represents an equivalence to physical inertia for distributed control in multi-agent dynamics.

B. Effective Inertia of a Cyber-Physical Agent

Evaluation of distributed control performance for transient stability has relied largely on numerical measures such as stability time [7]. Here, we formulate a setup of ESS-based distributed control as an equivalent synchronous machine to help arrive at insights on applied control and virtual inertia. This would be useful to address problems such as ESS placement and sizing. We build on the multi-agent representation in Section I to investigate the concept of inertia for cyber-physical agents. Let Agent i include the components of both Generator i and its associated ESS (denoted ESS$_i$) that is actuated with control signal u_i. We utilize the models in (8), (10), and (22) to gain an understanding of the impact of distributed control on the effective inertia of system agents. Let $\hat{H}_{\text{eff},i}(t)$ denote the effective inertia of Agent i as a result of the control action at time t (i.e., $u_i(t)$).

To arrive at a measure of the effective inertia $\hat{H}_{\text{eff},i}$, we compare the dynamics of Agent i as a function of H_i and u_i with that of an equivalent Generator i with the effect of the control u_i embedded in its effective inertia $\hat{H}_{\text{eff},i}$. As depicted in Fig. 1, the impact of the controlled storage can be interpreted as changing the effective inertia of a synchronous generator to achieve the same structure of dynamics. Consequently, the value of $\dot{\omega}_i(t)$ has to be the same for both the controlled agent and the equivalent generator. Thus, following (8) and (10), we find:

$$\begin{aligned}\dot{\omega}_i(t) &= \frac{\omega_s}{2H_i}(P_{Ai}(t) - D_i(\omega_i(t) - \omega_s) + u_i(t)) \\ &= \frac{\omega_s}{2\hat{H}_{\text{eff},i}(t)}(P_{Ai}(t) - D_i(\omega_i(t) - \omega_s)) \end{aligned} \tag{13}$$

which leads to:

$$\hat{H}_{\text{eff},i}(t) = H_i \frac{P_{Ai}(t) - D_i(\omega_i(t) - \omega_s)}{P_{Ai}(t) - D_i(\omega_i(t) - \omega_s) + u_i(t)}. \tag{14}$$

Consequently,

$$\hat{H}_{\text{eff},i}(t) = H_i\left(1 - \frac{u_i(t)}{P_{Ai}(t) - D_i(\omega_i(t) - \omega_s) + u_i(t)}\right) \tag{15}$$

is a measure of the effective inertia of the equivalent generator.

It is to be noted that usually $|P_{Ai}(t)| \gg D_i|\omega_i(t) - \omega_s|$ in typical transient stability studies, and so $P_{Ai}(t) - D_i(\omega_i(t) - \omega_s) \approx P_{Ai}(t)$; this leads to:

$$\frac{\hat{H}_{\text{eff},i}(t)}{H_i} \approx \frac{P_{Ai}(t)}{P_{Ai}(t) + u_i(t)}. \tag{16}$$

However, it is anticipated that the distributed controller will limit the effect of the accelerating power by injecting u_i that counters the value P_{Ai}; thus, it is very probable that $u_i(t)$ and $P_{Ai}(t)$ will have opposite signs. Consequently, it is expected that $|P_{Ai}(t) - D_i(\omega_i(t) - \omega_s) + u_i(t)| < |P_{Ai}(t)|$, and this means that $|\hat{H}_{\text{eff},i}(t)| \geq |H_i|$ in (14). Thus, compared to that of Generator i, the inertia of the effective generator of the cyber-physical agent is larger in magnitude. Within a transient stability perspective, high inertia is desirable as it prevents the power system from deviating quickly in response to a transient disturbance. This observation means that, analogous to the physical Generator i, the dynamics of the cyber-physical agent is slower to change during a disturbance and thus it can be considered more stable.

C. Virtual Inertia of an Actuated ESS

We now consider defining the virtual inertia of the actuated (i.e., controlled) ESS in isolation. The aggregate inertia of two synshronous generators depends on if the two machines are coherent or not [27]. Thus, the effective inertia of the cyber-physical agent is a combination of the generator inertia and the virtual inertia of the ESS. But, the ESS and associated synchronous generator are coherent since they share the same bus as shown in Fig. 2.

Thus, let $\hat{H}_{\text{ess},i}$ denote the virtual inertia of the actuated ESS$_i$. Then, the effective virtual inertia of the cyber-physical agent can be expressed as the sum of the virtual inertia of the ESS and the associated synchronous machine [27], [28]:

$$\hat{H}_{\text{eff},i}(t) = H_i + \hat{H}_{\text{ess},i}(t). \tag{17}$$

Equivalently, the virtual inertia constant can be expressed as:

$$\hat{H}_{\text{ess},i}(t) = \hat{H}_{\text{eff},i}(t) - H_i. \tag{18}$$

Utilizing (14), this can be calculated using:

$$\hat{H}_{\text{ess},i}(t) = H_i\left(\frac{P_{Ai}(t) - D_i(\omega_i(t) - \omega_s)}{P_{Ai}(t) - D_i(\omega_i(t) - \omega_s) + u_i}\right) - H_i. \quad (19)$$

Simplifying results in:

$$\hat{H}_{\text{ess},i}(t) = H_i \frac{-u_i(t)}{P_{Ai}(t) - D_i(\omega_i(t) - \omega_s) + u_i(t)}. \quad (20)$$

Recall that in transient stability studies it is usually the case that $|P_{Ai}(t)| \gg D_i|\omega_i(t) - \omega_s|$; thus, $P_{Ai}(t) - D_i(\omega_i(t) - \omega_s) \approx P_{Ai}(t)$. Consequently, the effective virtual inertia ratio can be approximated as:

$$\frac{\hat{H}_{\text{ess},i}(t)}{H_i} \approx \frac{-u_i(t)}{P_{Ai}(t) + u_i(t)}. \quad (21)$$

D. Observations

It is noted that when the distributed control is not activated for Generator i, i.e., $u_i = 0$, the effective inertia constant of the cyber-physical agent is equal to that of the physical generator as seen in (15); without the distributed control, the cyber-physical agent is effectively equivalent to the synchronous generator. Further, mimicking an open circuit, the virtual inertia constant of the actuated ESS appears as zero when the control power is zero as confirmed by (20), i.e., ESS is not contributing to stability. As the controller starts to stabilize the power grid and the rotor speed of Agent i approaches stability ($\omega_i \to \omega_s$ at stability), the control power of the agent approaches $-P_{Ai}(t)$. Thus, $|\hat{H}_{\text{eff},i}| \to \infty$ and $|\hat{H}_{\text{ess},i}| \to \infty$. Consequently, the actuated ESS dominates the dynamics of the Agent i, where no fluctuations will affect of the cyber-physical agent state.

E. Applications

The proposed framework arrives at an analytical expression for the effective inertia that is function of various attributes, which facilitates a variety of studies. As an example, since the effective inertia is implicitly a function of the actuated ESS capacity, an optimization framework would enable system operators to design the placement and sizing of ESS installed in a power system for a desired dynamical response. A possible deployment strategy can be investigated where synchronous generator with lower inertia are augmented with controlled ESS to enhance the power system dynamical response.

IV. Feedback Linearization Control

We extend our treatment to the ESS-based PFL control. PFL is a state-of-the-art distributed control for transient stability applications; it has a simple design, is parametric and tunable, allows for tractable analysis and can well accommodate communication delays and cyber attacks.

A. PFL Control

Consider the case of PFL control where the distributed controller actuates the output of ESS$_i$ to address transient stability according to:

$$u_i(t) = \begin{cases} C_i & \hat{u}_i(t) > C_i \\ \hat{u}_i(t) & -C_i \le \hat{u}_i(t) \le C_i \\ -C_i & \hat{u}_i(t) < -C_i \end{cases} \quad (22)$$

where C_i denotes the capacity of ESS$_i$ and:

$$\hat{u}_i(t) = -P_{Ai}(t) - \alpha_i(\omega_i(t) - \omega_s) \quad (23)$$

is the preprocessed control signal and $\alpha_i \ge 0$ is denoted as the speed stability parameter. This arrangement accommodates the case of limited storage capacity at Generator i as the control actuation cannot exceed capacity.

Next, expanding on the different values of $u_i(t)$ in (14) and (20), different cases of PFL control are considered.

B. Inertia With PFL Control

Given the structure of the PFL controller in (22), the effective inertia of the cyber-physical agent can be expressed as:

$$\frac{\hat{H}_{\text{eff},i}(t)}{H_i} = \begin{cases} \dfrac{P_{Ai}(t) - D_i(\omega_i(t) - \omega_s)}{P_{Ai}(t) - D_i(\omega_i(t) - \omega_s) + C_i} & \hat{u}_i(t) > C_i \\ \dfrac{P_{Ai}(t) - D_i(\omega_i(t) - \omega_s)}{P_{Ai}(t) - D_i(\omega_i(t) - \omega_s) - C_i} & \hat{u}_i(t) < -C_i \\ -\dfrac{P_{Ai}(t) - D_i(\omega_i(t) - \omega_s)}{(D_i + \alpha_i)(\omega_i(t) - \omega_s)} & \text{otherwise} \end{cases} \quad (24)$$

and the effective inertia constant of the actuated ESS$_i$ is found to be:

$$\frac{\hat{H}_{\text{ess},i}(t)}{H_i} = \begin{cases} \dfrac{-C_i}{P_{Ai}(t) - D_i(\omega_i(t) - \omega_s) + C_i} & \hat{u}_i(t) > C_i \\ \dfrac{C_i}{P_{Ai}(t) - D_i(\omega_i(t) - \omega_s) - C_i} & \hat{u}_i(t) < -C_i \\ \dfrac{P_{Ai}(t) + \alpha_i(\omega_i(t) - \omega_s)}{-D_i(\omega_i(t) - \omega_s) - \alpha_i(\omega_i(t) - \omega_s)} & \text{otherwise} \end{cases} \quad (25)$$

where $\hat{u}_i(t)$ is defined in (23), and $C_i \ge 0$ is the capacity of the storage unit in Agent i.

In the following we investigate the three possible cases of the control power range.

1) $\hat{u}_i(t) > C_i$: In this case the preprocessed control signal exceeds the ESS capacity limit, and thus the control signal is bounded to the maximum (i.e., $u_i(t) = C_i$). Usually $|P_{Ai}(t)| \gg |\omega_i(t) - \omega_s|$ and that it is very likely that $P_{Ai}(t) < 0$, and so this means that $P_{Ai}(t) + C_i < 0$. Accordingly, $\hat{H}_{\text{eff},i}(t)$ and $\hat{H}_{\text{ess},i}(t)$ are estimated as:

$$\begin{aligned} \frac{\hat{H}_{\text{eff},i}(t)}{H_i} &\approx \frac{P_{Ai}(t)}{P_{Ai}(t) + C_i} \\ \frac{\hat{H}_{\text{ess},i}(t)}{H_i} &\approx \frac{-C_i}{P_{Ai}(t) + C_i}. \end{aligned} \quad (26)$$

Since $|P_{Ai}(t)| > |P_{Ai}(t) + C_i|$, then $\hat{H}_{\text{eff},i}(t) > H_i$. Furthermore, since $P_{Ai}(t)$ and C_i have opposing signs, then $\hat{H}_{\text{ess},i}(t) > 0$. As the ESS capacity limit C_i increases, the magnitudes of $\hat{H}_{\text{eff},i}(t)$ and $\hat{H}_{\text{ess},i}(t)$ become smaller (resembling the case of high control power); however, increasing C_i means this case becomes

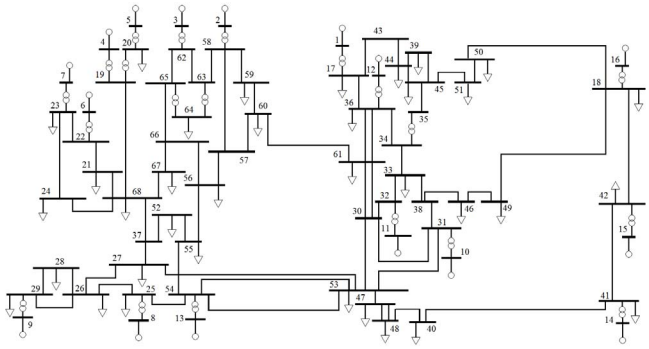

Fig. 3. Single line diagram of the IEEE 68-bus 16-machine test system.

less likely. On the other hand, decreasing the ESS limit to zero leads $\hat{H}_{\text{eff},i}(t)$ to approach H_i while $\hat{H}_{\text{ess},i}(t)$ becomes zero, similar to the case of zero control power.

2) $-C_i \le \hat{u}_i(t) \le C_i$*:* In this case the control signal equals the preprocessed one. Consequently, the effective inertia constant of the cyber-physical agent and the virtual inertia constant of the actuated ESS_i can be approximated as:

$$\frac{\hat{H}_{\text{eff},i}(t)}{H_i} \approx -\frac{P_{Ai}(t)}{(D_i+\alpha_i)(\omega_i(t)-\omega_s)}$$
$$\frac{\hat{H}_{\text{ess},i}(t)}{H_i} \approx -\frac{P_{Ai}(t)+\alpha_i(\omega_i(t)-\omega_s)}{(D_i+\alpha_i)(\omega_i(t)-\omega_s)}. \quad (27)$$

It can be observed that when $\omega_i(t) - \omega_s > 0$, the effective inertia of the cyber-physical agent is negative. Further, when $\omega_i(t) - \omega_s \to 0$, the virtual inertia of the actuated ESS is approximately the negative of the inertia constant of the synchronous machine, and the effective inertia constant approaches $\pm\infty$ depending on the sign of $P_{Ai}(t)$; thus making $\dot{\omega}_i(t) \to 0$, indicating the state of the cyber-physical agent is indifferent to any disturbance. Furthermore, increasing the ESS limit means this case becomes more likely.

3) $\hat{u}_i(t) < -C_i$*:* Here, $-P_{Ai} - \alpha_i(\omega_i - \omega_s) < -C_i$, and in this case the control signal is $u_i(t) = -C_i$. Here it is very probable in this case that $P_{Ai}(t) > 0$, and consequently $P_{Ai}(t) - C_i > 0$. Thus, the ratio of inertia constants are approximated for this case as:

$$\frac{\hat{H}_{\text{eff},i}(t)}{H_i} \approx \frac{P_{Ai}(t)}{P_{Ai}(t)-C_i}$$
$$\frac{\hat{H}_{\text{ess},i}(t)}{H_i} \approx \frac{C_i}{P_{Ai}(t)-C_i}. \quad (28)$$

Given that $P_{Ai}(t) > P_{Ai}(t) - C_i$, then $\hat{H}_{\text{eff},i}(t) > H_i$ and $\hat{H}_{\text{ess},i}(t) > 0$. In addition, increasing the value of C_i has similar consequences to that of the first case.

V. Numerical Results

The IEEE New York-New England test power system (also called the Northeast Power Coordinating Council (NPCC) power system) is used for numerical simulations. The test system has 16 conventional synchronous generators, 68 high-voltage buses, 66 transmission lines, and 35 loads as shown in Fig. 3. The parameters of this power system are extracted from [29], each generator is represented by (1)–(7), and the simulation environment follows the guidelines in [21]. More details about this test system can be found in [30].

A. Illustrative Example

In the test system described, a three-phase fault occurs at Bus 60 at $t = 1$ second for 5 cycles. The distributed PFL controller is activated immediately with $\alpha_i = 25$, and the capacity of each ESS in the system is limited as $C_i = 5\%P_{Mi}$. Sensors take periodic readings of the rotor speed and angle. The measurements are communicated to different agents where P_{Ai} is evaluated according to (7) and $P_{Ai} = P_{Mi} - P_{Ei}$. Then the PFL control calculates u_i based on P_{Ai} and the local rotor speed as shown in (22). The results for Agent 8 (synchronous Generator 8 and ESS_8) are shown in Fig. 4 as a demonstration; however, similar results can be observed for other generators in the system.

The performance of the PFL control is depicted in Fig. 4, where it can be observed how the system transient response was enhanced through the rotor speed and the relative rotor angle, and as is reflected by the power angle-based stability index η. The following general observations can be learned from the numerical results reported in Fig. 4:

- Initially, before the fault occurs, $\omega_i(t) = \omega_s$ and $P_{Ai}(t) = 0$; thus, the control power $u_i = 0$. Consequently, $\hat{H}_{\text{eff},i}(t) = H_i$ and $|\hat{H}_{\text{ess},i}(t)| = 0$.
- Shortly after the occurrence of the fault, the values of $P_{Ai}(t)$ fluctuate for few seconds; however, the control signal is limited to the capacity of the ESS. Thus, $\omega_i(t)$ swings around ω_s, and the values of $\hat{H}_{\text{eff},i}(t)$ and $\hat{H}_{\text{ess},i}(t)$ fluctuate as well following (15) and (20), respectively.
- Later, as $|\omega_i(t) - \omega_s| \to 0$, the generator is stabilizing and the value of the control signal approaches the negative of the accelerating power; i.e., $u_i(t) \approx -P_{Ai}(t)$. Accordingly, $|\hat{H}_{\text{eff},i}(t)| \to \infty$ and $|\hat{H}_{\text{ess},i}(t)| \to \infty$ as predicted in (16) and (21).

Eventually when other controls mechanisms such as governors are functioning $u_i \to 0$ and $|\hat{H}_{\text{eff},i}(t)| \to 0$ $|\hat{H}_{\text{ess},i}(t)| \to 0$ as discussed in Section II-B. It can be observed that the effective inertia of the agent characterized by $\hat{H}_{\text{eff},i}$ is dominated by the actuated storage virtual inertia $\hat{H}_{\text{ess},i}$. As shown, the inertia ratio for the effective inertia when $u_i = 0$ is 1, meanwhile the inertia ratio of virtual inertial of the actuated storage is 0 when $u_i = 0$. Otherwise, the main characteristics and behavior is very similar. A more detailed discussion of the impact of ESS capacity, PFL parameter, and communication delay follows.

B. Effect of ESS Capacity

We study the impact of varying the ESS capacity limit C_i in (22). Three different values of C_i are examined as $C_i = 1\%P_{Mi}$, $C_i = 10\%P_{Mi}$, and $C_i = 25\%P_{Mi}$. The simulation results are shown in Fig. 5. As can be observed, increasing the ESS capacity has obvious implications on the proposed inertia measures. For example, as C_i gets larger, it is more probable that $u_i = \hat{u}_i$, and consequently the effective inertia values are calculated using (27). This would result in a behavior where rapid changes in $\omega_i(t)$ greatly affect the effective

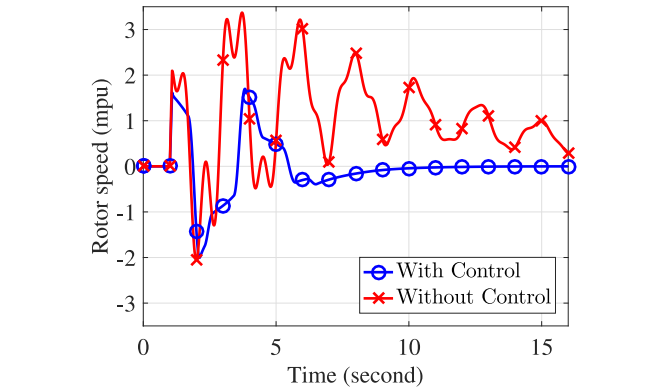

(a) Relative rotor speed

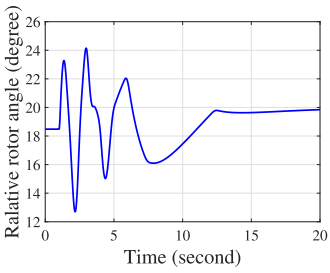

(b) Relative rotor angle

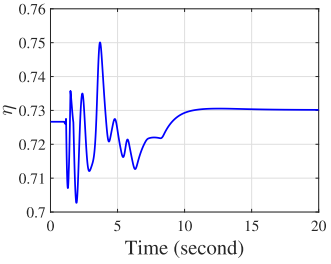

(c) Power angle-based stability index η

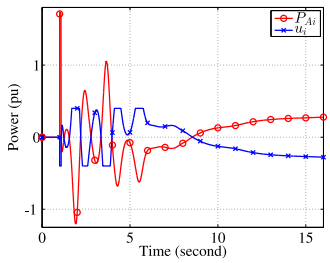

(d) Accelerating and control powers

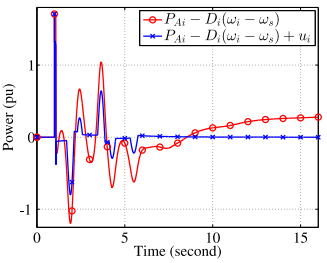

(e) Power values

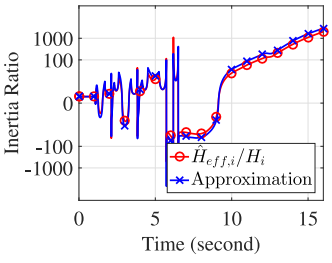

(f) $\hat{H}_{\text{eff},8}(t)$

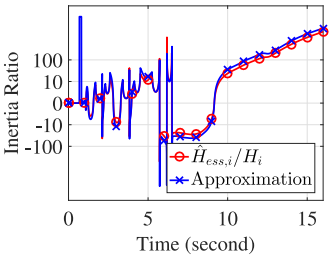

(g) $\hat{H}_{\text{ess},8}(t)$

Fig. 4. Results for Agent 8.

inertia measures. Hence, the values of $\hat{H}_{\text{eff},i}(t)$ and $\hat{H}_{\text{ess},i}(t)$ fluctuate more, but for a shorter duration; thus, $|\hat{H}_{\text{eff},i}(t)| \to \infty$ and $\hat{H}_{\text{ess},i}(t) \to \infty$ earlier.

C. Effect of PFL Speed Stability Parameter

Next, we study the impact of varying the PFL stability parameter α_i in (23). Three different values of the parameter are examined as $\alpha_i = D_i$, $\alpha_i = 5D_i$, and $\alpha_i = 10D_i$. Simulation results on the test system are shown in Fig. 6. The PFL control scheme is parametric through the speed stability parameter α. Increasing the value of α_i yields a more aggressive controller for ESS$_i$. As such, it is shown that higher values of α_i will result in a faster stability and an earlier time to achieve $|\hat{H}_{\text{eff},i}(t)| \to \infty$ and $\hat{H}_{\text{ess},i}(t) \to \infty$, and this is similar to the case of a higher ESS capacity.

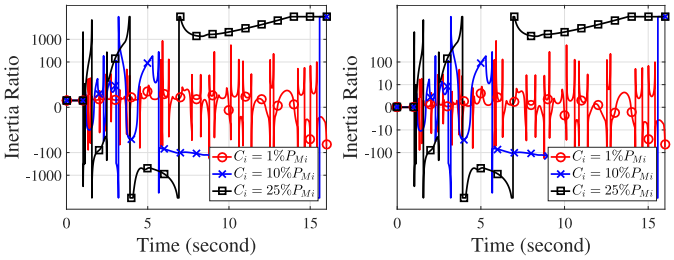

(a) Agent effective inertia (b) ESS virtual inertia

Fig. 5. Impact of ESS capacity on inertia measures of Agent 8.

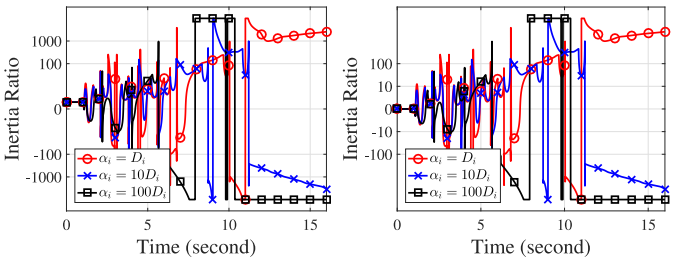

(a) Agent effective inertia (b) ESS virtual inertia

Fig. 6. Impact of controller parameter on inertia measures of Agent 8.

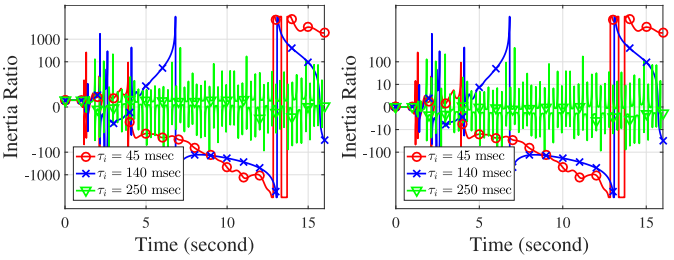

(a) Agent effective inertia (b) ESS virtual inertia

Fig. 7. Impact of communication delay on inertia measures constants of Agent 8.

D. Effect of Communication Delay

Finally, we consider the effect of communication delay (denoted τ) on the proposed measures. Communication delay impacts system measurements that are used to calculate $P_{Ai}(t)$ and thus indirectly affects effective inertia values. The different delay values examined are $\tau = 45$, $\tau = 140$, $\tau = 250$ msec, where the simulation results are shown in Fig. 7. Measurement latency results in a delayed corrective reaction from the PFL control in comparison to the evolving state of the system. As expected, it is shown that for a considerable range of delays, the PFL control is able to achieve $|\hat{H}_{\text{eff},i}(t)| \to \infty$ and $\hat{H}_{s,i}(t) \to \infty$. Whereas for high delays, for example $\tau = 250$ msec, the PFL control is not able to stabilize the system, where both $\hat{H}_{\text{eff},i}(t)$ and $\hat{H}_{\text{ess},i}(t)$ do not settle on desired values.

E. ESS-Based Control: A Remedial Control

The main goal of ESS-based distributed control addressing transient stability is to act as a remedial action till other control mechanisms such as exciters and governors intervene to actuate system operation. The ESS-based control enhances the transient response by modifying the dynamics of the generator such that the combined system, of the controlled ESS and the synchronous machine, has a zero net accelerating power. Nonetheless, the ESS-based control does not eliminate the difference between input mechanical power and output electrical power of the generator. Hence, if the power system is in a state where it is balanced by the persistent action of the controlled ESS, secondary control mechanisms such as governors will act based on their respective time constants to actuate the mechanical power to match the electric power of each generator, consequently driving the accelerating power P_{Ai} term to zero, and the controlled ESS control power to zero.

F. Discussion

The evolving smart grid with added storage, ESS, sensory, communication and distributed control motivate the advent of new measures to evaluate the performance of added system components. Within the multi-agent perspective of the power system with added ESS-based distributed control, the proposed effective virtual inertia measures arrive at analytical expressions describing the dynamical behavior of the cyber-physical control agent as in Equations (15)–(16) and (19)–(20).

As can be observed from previous numerical results, the proposed effective agent inertia $\hat{H}_{\text{eff},i}$ and actuated ESS virtual inertia $\hat{H}_{\text{ess},i}$ provide a useful tool in the analysis of ESS-based distributed control, where practical insights can be obtained from the analytical expression. For the case of PFL control, the effect of storage capacity on the effective virtual inertia of the control agent can be examined, where increased storage capacity results in decreased values of $\hat{H}_{\text{eff},i}$ and $\hat{H}_{\text{ess},i}$. Similar behavior is noticed for the impact of speed stability control parameters α_i, where a higher α_i results in faster dynamics. The proposed measures also facilitate the study of the impact of the communication delay of the measurements on the dynamics of the cyber-physical agents.

An expression of the proposed measures can be derived for the ESS-based controller of interest, hence identifying appropriate control strategies for power transmission systems. Further, the proposed effective virtual inertia measures enable tractable studies of storage capacity planning based on control architecture and design. Where for a desired transient stability dynamics of the overall power system, the capacity and location of the ESS and its associated control parameters can be optimized using the proposed effective inertia measures. Future extensions of this work will consider deriving the proposed measures of control agents for other power system stability studies.

VI. Conclusion

In this work we investigate storage-based distributed control for transient stability in power systems. Within a multi-agent framework, we propose an effective virtual inertia constant for cyber-physical agents and for the actuated ESSs. We present analytical expressions for the proposed measures for the case of a general ESS-based control. We extend the analysis for the distributed parametric feedback linearization control. Further, the proposed effective inertia measures are evaluated using the IEEE 68-bus test power system, where the impact of storage capacity, control parameters, and communication delay on the proposed inertia constants is shown. The proposed effective inertia constants facilitate an understanding of the impact of ESS-based distributed control and its various parameters from the perspective of traditional power systems for transient stability applications.

References

[1] P. Kundur *et al.*, "Definition and classification of power system stability IEEE/CIGRE joint task force on stability terms and definitions," *IEEE Trans. Power Syst.*, vol. 19, no. 3, pp. 1387–1401, Aug. 2004.

[2] J. Machowski, J. Bialek, and J. Bumby, *Power System Dynamics: Stability and Control*, 2nd ed. Hoboken, NJ, USA: Wiley, 2008.

[3] A. K. Farraj, E. M. Hammad, and D. Kundur, "A cyber-enabled stabilizing controller for resilient smart grid systems," in *Proc. IEEE PES Conf. Innov. Smart Grid Technol. (ISGT)*, Washington, DC, USA, Feb. 2015, pp. 1–5.

[4] P. Mercier, R. Cherkaoui, and A. Oudalov, "Optimizing a battery energy storage system for frequency control application in an isolated power system," *IEEE Trans. Power Syst.*, vol. 24, no. 3, pp. 1469–1477, Aug. 2009.

[5] J. Wei, D. Kundur, T. Zourntos, and K. L. Butler-Purry, "A flocking-based paradigm for hierarchical cyber-physical smart grid modeling and control," *IEEE Trans. Smart Grid*, vol. 5, no. 6, pp. 2687–2700, Nov. 2014.

[6] E. Hammad, A. Farraj, and D. Kundur, "Paradigms and performance of distributed cyber-enabled control schemes for the smart grid," in *Proc. IEEE Power Energy Soc. Gener. Meeting (PESGM)*, Denver, CO, USA, 2015, pp. 1–5.

[7] A. Farraj, E. Hammad, and D. Kundur, "A cyber-enabled stabilizing control scheme for resilient smart grid systems," *IEEE Trans. Smart Grid*, vol. 7, no. 4, pp. 1856–1865, Jul. 2016.

[8] P. Tielens and D. Van Hertem, "Grid inertia and frequency control in power systems with high penetration of renewables," in *Proc. Young Res. Symp. Elect. Power Eng.*, 2012, pp. 1–6.

[9] J. Driesen and K. Visscher, "Virtual synchronous generators," in *Proc. IEEE Power Energy Soc. Gener. Meeting Convers. Del. Elect. Energy 21st Century*, Pittsburgh, PA, USA, 2008, pp. 1–3.

[10] Q.-C. Zhong and G. Weiss, "Synchronverters: Inverters that mimic synchronous generators," *IEEE Trans. Ind. Electron.*, vol. 58, no. 4, pp. 1259–1267, Apr. 2011.

[11] H. Bevrani, T. Ise, and Y. Miura, "Virtual synchronous generators: A survey and new perspectives," *Int. J. Elect. Power Energy Syst.*, vol. 54, pp. 244–254, Jan. 2014.

[12] M. Torres, L. A. C. Lopes, L. Morán, and J. Espinoza, "Self-tuning virtual synchronous machine: A control strategy for energy storage systems to support dynamic frequency control," *IEEE Trans. Energy Convers.*, vol. 29, no. 4, pp. 833–840, Dec. 2014.

[13] M. Torres and L. A. Lopes, "An optimal virtual inertia controller to support frequency regulation in autonomous diesel power systems with high penetration of renewables," in *Proc. Int. Conf. Renew. Energies Power Qual. (ICREPQ)*, Las Palmas, Spain, 2011, pp. 959–964.

[14] E. Rakhshani, D. Remon, A. M. Cantarellas, and P. Rodriguez, "Analysis of derivative control based virtual inertia in multi-area high-voltage direct current interconnected power systems," *IET Gener. Transm. Distrib.*, vol. 10, no. 6, pp. 1458–1469, Apr. 2016.

[15] N. Soni, S. Doolla, and M. C. Chandorkar, "Improvement of transient response in microgrids using virtual inertia," *IEEE Trans. Power Del.*, vol. 28, no. 3, pp. 1830–1838, Jul. 2013.

[16] J. Alipoor, Y. Miura, and T. Ise, "Stability assessment and optimization methods for microgrid with multiple VSG units," *IEEE Trans. Smart Grid*, to be published.

[17] J. Alipoor, Y. Miura, and T. Ise, "Power system stabilization using virtual synchronous generator with alternating moment of inertia," *IEEE J. Emerg. Sel. Topics Power Electron.*, vol. 3, no. 2, pp. 451–458, Jun. 2015.

[18] P. Kundur, *Power System Stability and Control* (EPRI Power System Engineering Series). New York, NY, USA: McGraw-Hill, 1994.
[19] P. Anderson and A. Fouad, *Power System Control and Stability* (IEEE Power Systems Engineering Series). Piscataway, NJ, USA: IEEE Press, 1994.
[20] F. Dörfler and F. Bullo, "Kron reduction of graphs with applications to electrical networks," *IEEE Trans. Circuits Syst. I, Reg. Papers*, vol. 60, no. 1, pp. 150–163, Jan. 2013.
[21] P. W. Sauer and M. A. Pai, *Power System Dynamics and Stability*. Upper Saddle River, NJ, USA: Prentice-Hall, 1998.
[22] J. Glover, M. Sarma, and T. Overbye, *Power System Analysis & Design*, 5th ed. Boston, MA, USA: Cengage Learn., 2011.
[23] J. Berdy, "Out of step protection for generators," in *Proc. Georgia Inst. Technol. Protect. Relay Conf.*, 1976, pp. 1–26.
[24] D. A. Tziouvaras and D. Hou, "Out-of-step protection fundamentals and advancements," in *Proc. 57th Annu. Conf. Protect. Relay Eng.*, 2004, pp. 282–307.
[25] *TSAT: Transient Security Assessment Tool User Manual*, Powertech Labs Inc., Surrey, BC, Canada, Apr. 2011.
[26] M. Andreasson, D. Dimarogonas, H. Sandberg, and K. H. Johansson, "Distributed control of networked dynamical systems: Static feedback, integral action and consensus," *IEEE Trans. Autom. Control*, vol. 59, no. 7, pp. 1750–1764, Jul. 2014.
[27] J. J. Grainger and W. D. Stevenson, *Power System Analysis*. New York, NY, USA: McGraw-Hill, 1994.
[28] D. P. Kothari and I. Nagrath, *Modern Power System Analysis*. New Delhi, India: McGraw-Hill, 2003.
[29] B. Pal and B. Chaudhuri, *Robust Control in Power Systems* (Power Electronics and Power Systems Series). New York, NY, USA: Springer, 2005.
[30] A. K. Singh and B. C. Pal, "IEEE PES task force on benchmark systems for stability controls report on the 68-bus, 16-machine, 5-area system," IEEE Power Energy Soc., Chicago, IL, USA, Tech. Rep. 24, Dec. 2013.

Eman Hammad (S'14) received the B.Sc. degree from the University of Jordan and the M.Sc. degree from Texas A&M University, both in electrical engineering. She is currently pursuing the Ph.D. degree with the Department of Electrical Engineering, University of Toronto. Her current research interests include cyber-physical systems with particular interest in cyber-security, resilient control, and cooperative game theory in the context of smart grids. She was a recipient of many awards, and is currently serving as the IEEE Toronto Communication Society Chapter Chair.

Abdallah Farraj (S'11–M'12) received the B.Sc. and M.Sc. degrees in electrical engineering from the University of Jordan, Amman, Jordan, and the Ph.D. degree in electrical engineering from Texas A&M University, College Station, TX, USA. His research interests include modeling and analysis of cyber-physical systems, cyber security and resilience of smart grids, cognitive communications, and down-hole telemetry systems.

Deepa Kundur (S'91–M'99–SM'03–F'15) received the B.A.Sc., M.A.Sc., and Ph.D. degrees in electrical and computer engineering from the University of Toronto in 1993, 1995, and 1999, respectively. She is currently serves as the Chair of the Division of Engineering Science and as a Professor and the Director of the Centre for Power and Information, Edward S. Rogers Sr. Department of Electrical and Computer Engineering, University of Toronto, Toronto, Canada. From 2003 to 2012, she was a Faculty Member in electrical and computer engineering with Texas A&M University, and from 1999 to 2002, she was a Faculty Member in electrical and computer engineering with the University of Toronto.

Her research interests lie at the interface of cyber security, signal processing, and complex dynamical networks. She has authored over 150 journal and conference papers. She is also a recognized authority on cyber security issues and has appeared as an Expert in popular television, radio, and print media. She has participated on several editorial and conference executive boards, and currently serves on the Advisory Board of IEEE Spectrum.

Prof. Kundur was a recipient of best paper recognitions at numerous venues including the 2015 IEEE Smart Grid Communications Conference, the 2015 IEEE Electrical Power and Energy Conference, the 2012 IEEE Canadian Conference on Electrical & Computer Engineering, the 2011 Cyber Security and Information Intelligence Research Workshop, the 2008 IEEE INFOCOM Workshop on Mission Critical Networks, and the Teaching Awards at both the University of Toronto and Texas A&M University. She is a fellow of the Canadian Academy of Engineering.